Structural, mechanical, thermodynamic, and electronic properties of thorium hydrides from first principles

Bao-Tian Wang,[1,2] Ping Zhang,[2,3,*] Hongzhou Song,[2] Hongliang Shi,[2,4] Dafang Li,[2] and Wei-Dong Li[1]

[1] *Institute of Theoretical Physics and Department of Physics, Shanxi University, Taiyuan 030006, People's Republic of China*

[2] *LCP, Institute of Applied Physics and Computational Mathematics, Beijing 100088, People's Republic of China*

[3] *Center for Applied Physics and Technology, Peking University, Beijing 100871, People's Republic of China*

[4] *SKLSM, Institute of Semiconductors, Chinese Academy of Sciences, People's Republic of China*

We perform first-principles calculations of the structural, electronic, mechanical, and thermodynamic properties of thorium hydrides (ThH_2 and Th_4H_{15}) based on the density functional theory with generalized gradient approximation. The equilibrium geometries, the total and partial densities of states, charge density, elastic constants, elastic moduli, Poisson's ratio, and phonon dispersion curves for these materials are systematically investigated and analyzed in comparison with experiments and previous calculations. These results show that our calculated equilibrium structural parameters are well consistent with experiments. The Th−H bonds in all thorium hydrides exhibit weak covalent character, but the ionic properties for ThH_2 and Th_4H_{15} are different due to their different hydrogen concentration. It is found that while in ThH_2 about 1.5 electrons transfer from each Th atom to H, in Th_4H_{15} the charge transfer from each Th atom is around 2.1 electrons. Our calculated phonon spectrum for the stable body-centered tetragonal phase of ThH_2 accords well with experiments. In addition we show that ThH_2 in the fluorite phase is mechanically and dynamically unstable.

PACS numbers: 71.27.+a, 71.15.Mb, 71.20.-b, 63.20.dk

I. INTRODUCTION

Thorium is one kind of important nuclear materials and together with its compounds has been widely investigated both experimentally and theoretically. Among thorium compounds, thorium hydrides (ThH_2 and Th_4H_{15}) are metallic solids and have potential use for advanced nuclear fuels. In addition, Th_4H_{15} has been reported to have superconductivity with transition temperatures T_c $\sim$8 K[1] and has been considered as promising candidates for hydrogen storage since its large hydrogen-to-metal ratio[2]. ThH_2 is not superconducting above 1 K[3].

Despite the abundant research on thorium hydrides, relatively little is known regarding their chemical bonding, mechanical properties, and phonon dispersion. Only the optical phonon density of states of ThH_2 and Th_4H_{15} was measured through inelastic neutron scattering[4] and the bulk modulus of ThH_2 was calculated by linear muffin-tin orbital (LMTO) method[5]. Until now the elastic properties, which relate to various fundamental solid-state properties such as interatomic potentials, equation of state, phonon spectra, and thermodynamical properties, are unknown for ThH_2 and Th_4H_{15}. In addition, although the electronic properties as well as the chemical bonding in thorium hydrides have been calculated recently by Shein *et al.*[2] through the full-potential LAPW (FLAPW) method, the study of the bonding nature of Th−H bond involving its mixed ionic/covalent character is still lacking. These facts, as a consequence, inhibit deep understanding of thorium hydrides. Motivated by these observations, in this paper, we present a first-principles study by calculating the structural, electronic, mechanical, and thermodynamic properties of thorium hydrides. Also, the stability of the metastable phase of ThH_2 (fluorite structure with space group $Fm\bar{3}m$) is analyzed and our calculated results show that the fluorite-type ThH_2 is mechanically unstable. We perform the Bader analysis[6,7] of thorium hydrides and find that about 1.5 (2.1) electrons transfer from each Th atom to H for ThH_2 (Th_4H_{15}).

II. COMPUTATIONAL METHODS

Our total energy calculations are carried out by employing the plane-wave basis pseudopotential method as implemented in Vienna *ab initio* simulation package (VASP)[8]. The exchange and correlation effects are described by the density functional theory (DFT) within generalized gradient approximation (GGA)[9]. The projected augmented wave (PAW) method of Blöchl[10] is implemented in VASP with the frozen-core approximation. The thorium $6s^2 7s^2 6p^6 6d^1 5f^1$ and the hydrogen $1s^1$ electrons are treated as valence electrons. Note that although the $5f$ states are empty in elemental Th, this level turns to evolve into a hybridization with the hydrogen orbitals both in the valence band and the conduction band, as well as to prominently contribute to the conduction band (see Fig. 3 below). 9×9×9 and 5×5×5 Monkhorst-Pack[11] k point-meshes in the full wedge of the Brillouin zone are used for ThH_2 and Th_4H_{15}, respectively. Electron wave function is expanded in plane waves up to a cutoff energy of 450 eV, and all atoms are fully relaxed until the Hellmann-Feynman forces become less than 0.02 eV/Å.

In present work, the theoretical equilibrium volume,

bulk modulus B, and pressure derivative of the bulk modulus B' are obtained by fitting the energy-volume data in the third-order Birch-Murnaghan equation of state (EOS)[12]. In order to calculate elastic constants, a small strain is applied onto the structure. For small strain ϵ, Hooke's law is valid and the crystal energy $E(V,\epsilon)$ can be expanded as a Taylor series[13],

$$E(V,\epsilon) = E(V_0,0) + V_0 \sum_{i=1}^{6} \sigma_i e_i + \frac{V_0}{2} \sum_{i,j=1}^{6} C_{ij} e_i e_j + O(\{e_i^3\}), \quad (1)$$

where $E(V_0,0)$ is the energy of the unstrained system with the equilibrium volume V_0, ϵ is strain tensor which has matrix elements ε_{ij} (i,j=1, 2, and 3) defined by

$$\varepsilon_{ij} = \begin{pmatrix} e_1 & \frac{1}{2}e_6 & \frac{1}{2}e_5 \\ \frac{1}{2}e_6 & e_2 & \frac{1}{2}e_4 \\ \frac{1}{2}e_5 & \frac{1}{2}e_4 & e_3 \end{pmatrix} \quad (2)$$

and C_{ij} are the elastic constants. For cubic structures, there are three independent elastic constants (C_{11}, C_{12}, and C_{44}). So, the elastic constants for fcc ThH_2 and bcc Th_4H_{15} can be calculated from three different strains listed in the following:

$$\epsilon^1 = (\delta,\delta,\delta,0,0,0), \epsilon^2 = (\delta,0,\delta,0,0,0), \epsilon^3 = (0,0,0,\delta,\delta,\delta). \quad (3)$$

The strain amplitude δ is varied in steps of 0.006 from δ=−0.036 to 0.036 and the total energies $E(V,\delta)$ at these strain steps are calculated. After obtaining elastic constants, we can calculate bulk and shear moduli from the Voigt-Reuss-Hill (VRH) approximations[14–16]. The Voigt (Reuss) bounds on the bulk modulus B_V (B_R) and shear modulus G_V (G_R) for these two cubic crystal systems are deduced from the formulas of elastic moduli in Ref.[17]. As for bct ThH_2, the six independent elastic constants (C_{11}, C_{12}, C_{44}, C_{13}, C_{33}, and C_{66}) can be obtained from six different strains listed in the following:

$$\epsilon^1 = (\delta,\delta,\delta,0,0,0), \epsilon^2 = (\delta,0,\delta,0,0,0), \epsilon^3 = (\delta,\delta,0,0,0,0), \epsilon^4 = (0,0,\delta,0,0,0), \epsilon^5 = (0,0,0,\delta,\delta,0), \epsilon^6 = (0,0,0,0,0,\delta) \quad (4)$$

and the formulas of elastic moduli in VRH approximations[16] are from Ref.[18]. Based on Hill approximation[16], B=$\frac{1}{2}$($B_R + B_V$) and G=$\frac{1}{2}$($G_R + G_V$). The Young's modulus E and Poisson's ratio υ are given by the following formulas:

$$E = 9BG/(3B+G), \upsilon = (3B-2G)/[2(3B+G)]. \quad (5)$$

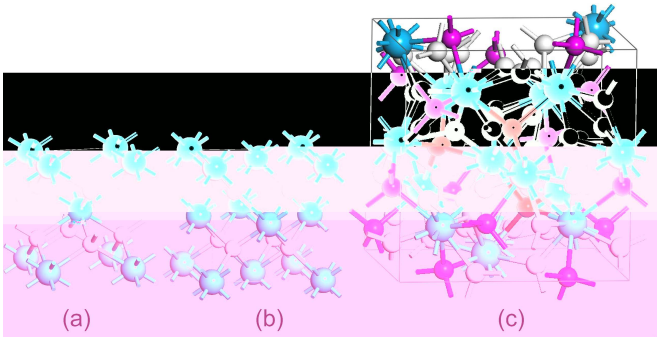

FIG. 1: (Color online) Crystal structures of (a) bct ThH_2, (b) fcc ThH_2, and (c) bcc Th_4H_{15}. Here, larger cyan spheres stand for Th atoms and the smaller white H. Note that the magenta and red spheres in (c) stand for H1 and the white and grey spheres H2.

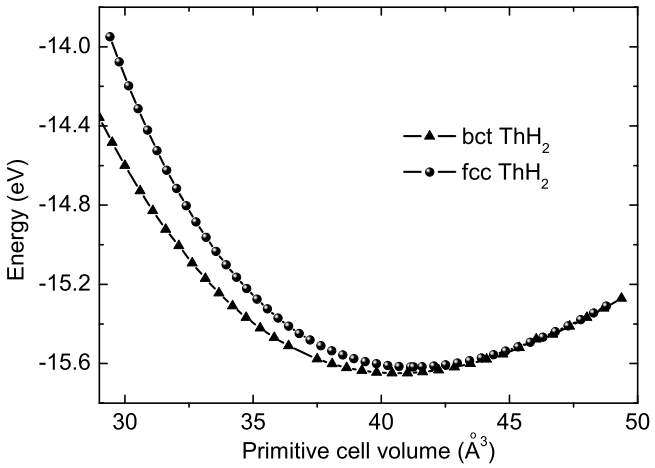

FIG. 2: Comparison of total energy vs the primitive cell volume for ThH_2 in bct and fcc phases.

III. RESULTS

A. Atomic and electronic structures of thorium hydrides

At ambient condition, the stable thorium dihydride crystallizes in a body-centered tetragonal (bct) ionic structure with space group $I4/mmm$ (No. 139). Its unit cell is composed of two ThH_2 formula units with the thorium atoms and the hydrogen atoms in $2a$ (in Wyckoff notation) and $4d$ sites, respectively [see Fig. 1(a)]. Each Th atom is surrounded by eight H atoms forming a tetragonal and each H connects with four Th atoms to build a tetrahedron. The present optimized lattice parameters (a and c) are 4.0670 Å and 4.9125 Å (see Table I), in good agreement with the experimental[19] values of 4.10 Å and 5.03 Å. Besides, the face-centered cubic (fcc) fluorite-type structure with space group $Fm\bar{3}m$

TABLE I: Optimized structural parameters, partial and total densities of states at the Feimi level $N(E_{\rm F})$ (states/eV/Th atom) for thorium hydrides. For comparison, other theoretical results and available experimental data are also listed.

Compound	Cell constants (Å)	Coordinates	Th 6d	Th 5f	H s	Total
bct ThH_2	a=4.0670 (4.0475)[a], (4.10)[c]	Th (2a): 0, 0, 0	0.383	0.165	0.002	0.996
(I4/mmm)	c=4.9125 (4.9778)[a], (5.03)[c]	H (4d): 0, 0.5, 0.25	(0.207)[a]	(0.140)[a]	(0.001)[a]	(0.866)[a]
fcc ThH_2	a=5.4851 (5.4902)[a], (5.489)[b]	Th (4a): 0, 0, 0	0.610	0.244	0.003	1.557
($Fm\bar{3}m$)		H (8c): 0.25, 0.25, 0.25	(0.374)[a]	(0.202)[a]	(0.002)[a]	(1.451)[a]
Th_4H_{15}	a=9.1304 (9.1280)[a], (9.11)[c,d]	Th (16c): x, x, x; x=0.2087 (0.208)[d]	0.610	0.678	0.031	2.334
($I\bar{4}3d$)		H1 (12a): 0.375, 0, 0.25	(0.441)[a]	(0.619)[a]	(0.049)[a]	(2.474)[a]
		H2 (48e): 0.372, 0.219, 0.404 (0.4, 0.23, 0.372)[d]				

[a] Reference[2], [b] Reference[5], [c] Reference[19], [d] Reference[20].

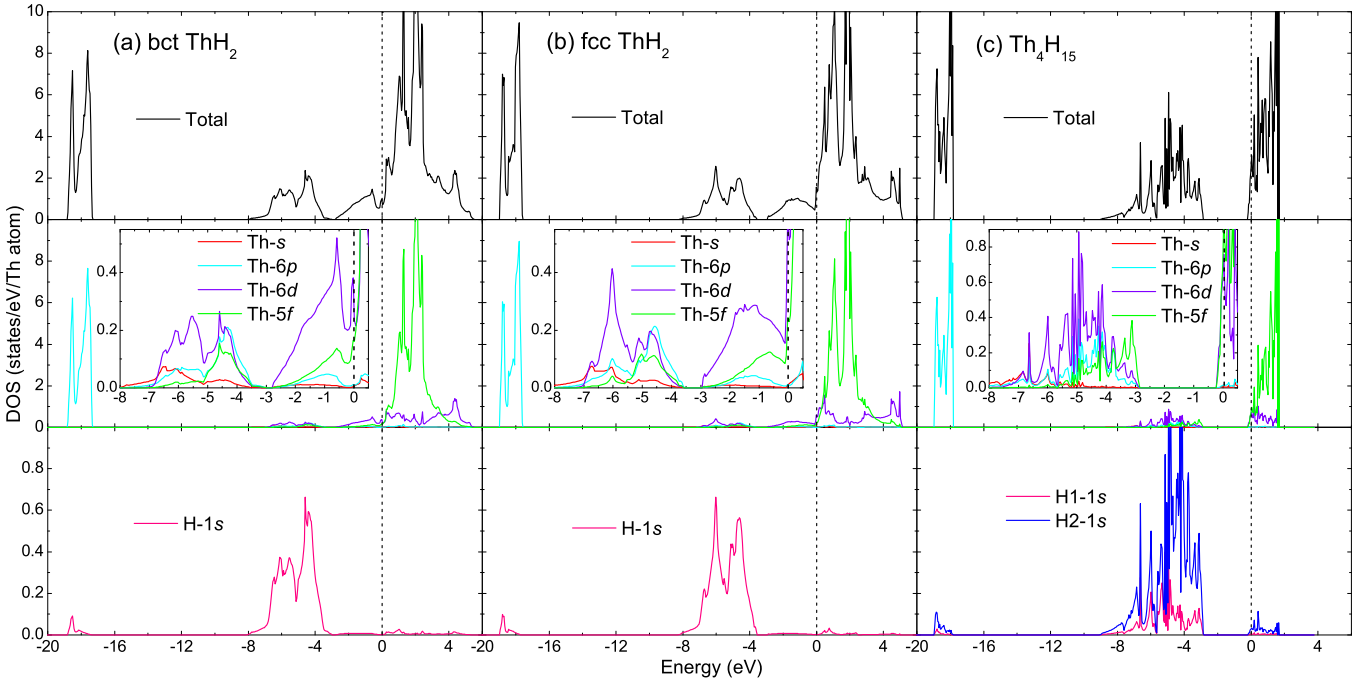

FIG. 3: (Color online) Total and orbital-resolved local densities of states for (a) bct ThH_2, (b) fcc ThH_2, and (c) bcc Th_4H_{15}. The Fermi energy level is set at zero.

(No. 225) is considered as metastable phase for ThH_2 [see Fig. 1(b)]. The fluorite structure is the stable structure of all actinide dioxides. Moreover, this fcc structure can be obtained from the bct stable structure by modulating the base vectors. In fcc structure, each Th atom is surrounded by eight H atoms forming a cube and each H connects with four Th atoms to build a tetrahedron. Our optimized lattice constant (a) for fcc ThH_2 is 5.4851 Å (see Table I), in excellent agreement with the measured[5] values of 5.489 Å. The structure of Th_4H_{15} is more complicated. It crystallizes in a body-centered cubic (bcc) structure with space group $I\bar{4}3d$ (No. 220) [see Fig. 1(c)]. The unit cell has sixteen Th (16c), twelve H1 (12a), and forty eight H2 (48e) atoms. Each H1 is surrounded by four Th atoms to build the tetrahedral structure and each H2 is located at the center of triangle formed by three Th atoms. As a result, each Th is surrounded by three H1 atoms and nine H2 atoms. In Fig. 1(c), we label clearly the H1 atoms (red spheres) and H2 atoms (grey spheres) connected to the Th atom located at center. The current optimized structural parameters of Th_4H_{15} are listed in Table I, where one can find that our calculation results are in good agreement with experiment[20].

To investigate the stability of ThH_2, we have optimized the structural parameters of its bct and fcc structures at different pressures. To avoid the Pulay stress problem, we perform the structure relaxation calculations at fixed volumes rather than constant pressures. For fcc structure, due to its high symmetry, the structure relaxation calculations are performed at fixed volumes with no relaxation of coordinates and cell shape. However, for bct structure, the cell shape is necessary to be optimized due

to their internal degrees of freedom. The total energies (per primitive cell) of the two structures at different volumes are calculated and shown in Fig. 2. Obviously, the bct ThH_2 is more stable than fcc ThH_2 under ambient pressure. The equilibrium volumes of bct and fcc structures are 40.63 Å^3 and 41.26 Å^3, respectively. Thus the equilibrium volumes of both bct and fcc phases are approximately equal and the total energy difference at their equilibrium states is ∼0.032 eV. This conclusion is consistent well with the previous FLAPW results[2].

Basically, all the macroscopical properties of materials, such as hardness, elasticity, and conductivity, originate from their electronic structure properties as well as chemical bonding nature. Therefore, it is necessary to perform the electronic structure analysis of thorium hydrides. The calculated total densities of states (DOS) and the orbital-resolved partial densities of states (PDOS) of bct ThH_2, fcc ThH_2 and bcc Th_4H_{15} are shown in Fig. 3. Overall, the occupation properties of ThH_2 in bct and fcc phases are similar. The occupied DOS near the Fermi level is featured by the three well-resolved peaks. The one near −1.0 eV is principally Th 6*d* in character, while the other two peaks respectively near −4.5 and −6.0 eV are mostly H 1*s* hybridized with Th 6*d* and Th 5*f* orbitals. These well-separated orbital peaks have been observed in the photoelectron spectroscopy (PES) measurement[21]. In addition, the band width of the Th 6*d* valence band near the Fermi level is 3 eV, consistent with the FLAPW calculation[2] and experimental data[21]. The H 1*s* valence band width is of 5.0 eV, also in accord with the experimental data (6.0 eV) and previous FLAPW result (5.2 eV). Moreover, the low bands of bct (fcc) ThH_2 covering from −18.8 (−19.0) to −17.2 (−17.5) eV is mainly featured by Th 6*p* state mixed with a little H 1*s* state and the conduction bands is principally occupied by Th 5*f* states with admixtures of the Th 6*d* and H 1*s* states and has a width of 5.5 (5.1) eV. For Th_4H_{15}, our calculations reproduce all the features calculated by Shein *et al.*[2] and agree well with PES measurements[21]. Note that our calculated conduction band width is 1.7 eV, consistent with the PES experimental value[21] (0.9 eV) and evidently smaller than that of FLAPW calculation result[2]. The main occupation of conduction bands is Th 5*f* orbital, mixed with a little Th 6*d* and H 1*s* states. In addition, we have also presented in Table I the partial and total DOSs at the Feimi level $N(E_F)$ for thorium hydrides to study the occupation of the conduction band. Clearly, our results are in good agreement with the FLAPW calculation[2].

In order to gain more insight into the bonding nature of ground state thorium hydrides, we also investigate the valence charge density distribution. The calculated valence charge density maps of the bct ThH_2 in (100) plane, fcc ThH_2 in $(1\bar{1}0)$ plane, and bcc Th_4H_{15} in plane established by three Th and one H2 atoms are plotted in Fig. 4. Clearly, the charge densities around Th and H ions are all near spherical distribution with slightly deformed towards the direction to their nearest neighboring atoms.

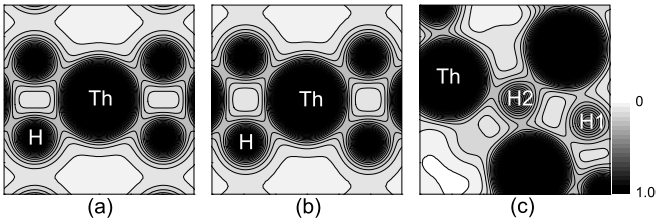

FIG. 4: Valence charge density of (a) bct ThH_2 in (100) plane, (b) fcc ThH_2 in $(1\bar{1}0)$ plane, and (c) bcc Th_4H_{15} in plane established by three Th and one H2 atoms. Contour lines are drawn from 0.0 to 1.0 at 0.05 e/Å^3 intervals.

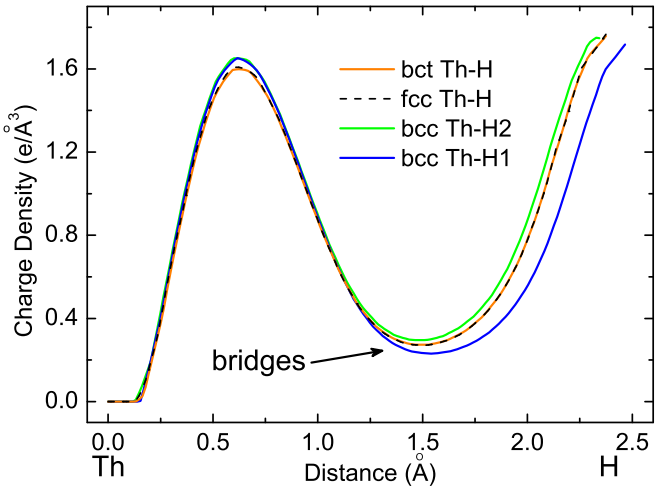

FIG. 5: (Color online) Line charge density distribution between Th atom and the nearest neighbor H atom for bct ThH_2, fcc ThH_2, and bcc Th_4H_{15}.

To describe the ionic/covalent character quantitatively and more clearly, we plot in Fig. 5 the line charge density distribution along the nearest Th−H bonds and perform the Bader analysis[6,7]. For bct and fcc ThH_2, the two charge density curves change with the same way along the Th−H bonds. For Th_4H_{15}, the two curves along the Th−H1 and Th−H2 bonds are almost the same before the bridge locus (indicated by the arrow), after where they split evidently. Besides, one can find a minimum value of charge density in Fig. 5 for each bond at around the bridge. These minimum values are listed in Table II. Although these values are much smaller than 0.7 e/Å^3 for Si covalent bond, they are prominently higher than 0.05 e/Å^3 for Na−Cl bond in typical ionic crystal NaCl. Also we notice that these values are smaller than the minimum values (0.45 e/Å^3) of charge density along the Th−O bond in our previous study of ThO_2[22]. Therefore, there are weak but clear covalent bonds between Th and H for ThH_2 in bct and fcc phases and for bcc Th_4H_{15}. The slight difference appears in Th_4H_{15}, where the minimum value of charge density in Th−H1 bond is smaller than that in Th−H2 bond. In addition, one can

TABLE II: Calculated charges and volumes according to Bader partitioning as well as the Th−H distances and correlated minimum values of charge densities along the Th−H bonds for thorium hydrides. As a comparison, other theoretical work and available experimental data are also listed. Note that some properties of Th_4H_{15} have two values (first for H1 and second for H2).

Compound	Q_B(Th) (e)	Q_B(H) (e)	V_B(Th) (Å^3)	V_B(H) (Å^3)	Th−H (Å)	Charge density$_{min.}$ (e/Å^3)
bct ThH_2	10.530	1.735	25.59	7.50	2.375 (2.385)[a]	0.273
fcc ThH_2	10.488	1.756	25.72	7.77	2.375 (2.337)[b]	0.271
Th_4H_{15}	9.870	1.590, 1.563	20.15	7.16, 7.35	2.465 (2.46)[a], 2.343 (2.29)[a]	0.231, 0.296

[a] Reference[19], [b] Reference[5].

notice from Table II that our calculated Th−H distances are all well consistent with the previous theoretical[5] and experimental[19] results. As for Bader analysis, it is a well established analysis tool for studying the topology of the electron density and thus is particularly suitable for discussing the mixed ionic/covalent character of a compound. The charge (Q_B) enclosed within the Bader volume (V_B) is a good approximation to the total electronic charge of an atom. In the present study, the default charge density grids for one unit cell are 56×56×72, 56×56×56, and 112×112×112 for bct ThH_2, fcc ThH_2, and bcc Th_4H_{15}, respectively. To check the precision, the charge density distribution for fcc ThH_2 is calculated with a series of n times finer grids (n = 2, 3, 4, 5, 6). The deviation of the effective charge between the five and the six times finer grids is less than 0.02%. Thus we perform the charge density calculations using the six times finer grid (336×336×432, 336×336×336, and 672×672×672 for bct ThH_2, fcc ThH_2, and bcc Th_4H_{15}, respectively). The calculated results are presented in Table II. Note that although we have included the core charge in charge density calculations, since we do not expect variations as far as the trends are concerned, only the valence charge are listed. From Table II the following prominent features can be seen: (i) The Bader charges and volumes for bct and fcc ThH_2 are almost equal to each other. This shows the same ionic character, through a flux of charge (about 1.5 electrons for each Th atom) from cations towards anions, for thorium dihydride both in their stable phase and metastable phase. (ii) The Bader charges and volumes for bcc Th_4H_{15} are different comparing to thorium dihydride. This originates from their different hydrogen concentration. For bcc Th_4H_{15}, about 2.1 electrons transfer from each Th atom to H. This indicates that the Th atoms in Th_4H_{15} are more ionized than that in thorium dihydrides.

B. Mechanical properties of thorium hydrides

Our calculated elastic constants, various moduli, pressure derivative of the bulk modulus $B^{'}$, and Poisson's ratio υ for bct ThH_2, fcc ThH_2, and bcc Th_4H_{15} are collected in Table III. Obviously, bct ThH_2 is mechanically stable due to the fact that its elastic constants satisfy the following mechanical stability criteria[23] of tetragonal structure:

$$\begin{aligned} C_{11}>0, C_{33}>0, C_{44}>0, C_{66}>0, \\ (C_{11}-C_{12})>0, (C_{11}+C_{33}-2C_{13})>0, \\ [2(C_{11}+C_{12})+C_{33}+4C_{13}]>0. \end{aligned} \quad (6)$$

Th_4H_{15} is also mechanically stable because its elastic constants satisfy the following mechanical stability criteria[23] of cubic structure:

$$C_{11}>0, C_{44}>0, C_{11}>|C_{12}|, (C_{11}+2C_{12})>0. \quad (7)$$

However, the ThH_2 in its metastable cubic phase is mechanically unstable. In fact, one can see from Table III that C_{11} is much smaller than C_{12} for fcc ThH_2. Therefore, the mechanical stability criteria[23] $C_{11}>|C_{12}|$ can not be satisfied and the shear modulus, Young's modulus, and Poisson's ratio also can not be obtained. As for bulk modulus B, each derived value from VRH approximations[16] for all the thorium hydrides turns out to be very close to that obtained by fitting Murnaghan EOS[12]. Moreover, we notice that our calculated B for fcc ThH_2 is approximately equal to previous LMTO theoretical result[5]. For shear modulus G and Young's modulus E, their values for bcc Th_4H_{15} are approximately 2.5 times of those for bct ThH_2. For Poisson's ratio, the values for both bct ThH_2 and bcc Th_4H_{15} are within the range from 0.25 to 0.45 for typical metals.

C. Phonon dispersion curves of thorium dihydrides

Employing the Hellmann-Feynman theorem and the direct method, we have calculated the phonon curves along some high-symmetry directions in the Brillouin zone (BZ), together with the phonon PDOS. For the phonon dispersion calculation, we use the 2×2×2 bct (fcc) supercell containing 48 (96) atoms for bct (fcc) ThH_2. To calculate the Hellmann-Feynman forces, we displace four and eight atoms, respectively, for bct and fcc ThH_2 from their equilibrium positions and the amplitude of all the displacements is 0.03 Å. The calculated phonon dispersion curves along the

TABLE III: Calculated elastic constants, various moduli, and Poisson's ratio υ for thorium hydrides.

Compound	C_{11} (GPa)	C_{12} (GPa)	C_{44} (GPa)	C_{13} (GPa)	C_{33} (GPa)	C_{66} (GPa)	B (GPa)	$B^{'}$ (GPa)	G (GPa)	E (GPa)	υ
bct ThH_2	131	100	29	78	89	5	91	3.3	16	44	0.419
fcc ThH_2	46	119	57				95 (99)[a]	3.8			
Th_4H_{15}	121	66	59				85	2.2	43	111	0.282

[a] Reference[5].

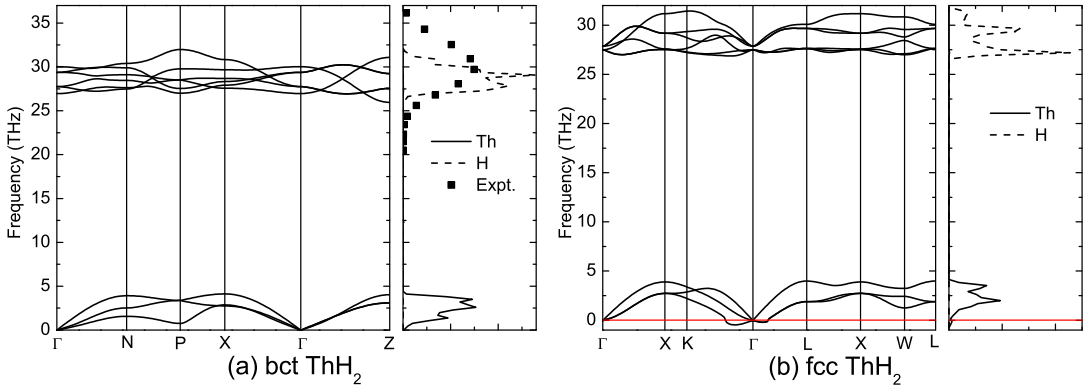

FIG. 6: (Color online) Calculated phonon dispersion curves and corresponding PDOS for (a) bct ThH_2 and (b) fcc ThH_2. For comparison, the experimental data in Ref. [4] are also shown (squares).

$\Gamma-N-P-X-\Gamma-Z$ directions for bct ThH_2 and along the $\Gamma-X-K-\Gamma-L-X-W-L$ directions for fcc ThH_2 are displayed in Fig. 6(a) and Fig. 6(b), respectively.

For both bct and fcc ThH_2, there are only three atoms in their primitive cells. Therefore, nine phonon modes exist in the dispersion relations. Due to the fact that thorium is much heavier than hydrogen atom, the vibration frequency of thorium atom is apparently lower than that of hydrogen atom. Therefore, evident gap between the optic modes and the acoustic branches exits and the phonon DOS of bct (fcc) ThH_2 can be viewed as two parts. One is the part lower than 4.4 (4.1) THz where the main contribution comes from the thorium sublattice, while the other part range from 26.0 to 32.1 (26.4 to 31.8) THz is dominated by the dynamics of the light hydrogen atoms. In experimental measurements, Dietrich *et al.* reported that the acoustic branches of ThH_2 are lower than 4.8 THz and optic modes range from 23.4 to 36.2 THz[4]. Their measured data of optic modes are presented in Fig. 6(a) for comparison and the acoustic-phonon data are unable obtained from their time-of-flight spectrum. Obviously, our calculated results are on the whole consistent with the experimental data. In addition, while all frequencies are positive for bct ThH_2, which assures a dynamical stability of the bct phase against mechanical perturbations. For fcc ThH_2, one can see from Fig. 6 (b) that the transverse acoustic (TA) mode close to Γ point becomes imaginary along the $\Gamma-K$ and $\Gamma-L$ directions. The minimum of the TA branch occurs along the $\Gamma-K$ direction. This indicates instability of fcc phase of ThH_2 compared to stable bct phase, which is well consistent with our previous mechanical stability analysis of ThH_2. Moreover, there exists LO-TO splitting at Γ point in bct phase. But in fcc phase there is no LO-TO splitting.

IV. CONCLUSION

In summary, we have used the first-principles DFT-GGA method to calculate the structural, electronic, mechanical, and thermodynamic properties of ThH_2 in its stable bct phase and metastable fcc phase and Th_4H_{15} in bcc phase. Our optimized structural parameters are well consistent with experiments. The occupation characters of electronic orbitals also accord well with experiments and previous calculations. Through Bader analysis, we have found that the Th−H bonds in all thorium hydrides exhibit weak covalent character, but the ionic property for ThH_2 and Th_4H_{15} are different. While ∼1.5 electrons transfer from each Th atom to H in ThH_2, in Th_4H_{15} about 2.1 electrons deviate from each Th atom. In addition, our calculated phonon curves of fcc ThH_2 have shown that the TA mode becomes imaginary close to Γ point and the subsequent instability of this phase.

Acknowledgments

This work was supported by the Foundations for Development of Science and Technology of China Academy

of Engineering Physics under Grants No. 2009B0301037 and No. 2009A0102005.

---

* Author to whom correspondence should be addressed. E-mail: zhang_ping@iapcm.ac.cn

[1] C. B. Satterthwaite and I. L. Toepke, Phys. Rev. Lett. **25**, 741 (1970).

[2] I. R. Shein, K. I. Shein, N. I. Medvedeva, and A. L. Ivanovskii, Physica B **389**, 296 (2007).

[3] C. B. Satterthwaite and D. T. Peterson, J. Less-Common Met. **26**, 361 (1972).

[4] M. Dietrich, W. Reichardt, and H. Rietschel, Solid State Commun. **21** 603 (1977).

[5] M. S. S. Brooks and B. Johansson, Physica B **130**, 516 (1985).

[6] R. F. W. Bader, *Atoms in Molecules: A Quantum Theory* (Oxford University Press, New York, 1990).

[7] W. Tang, E. Sanville, and G. Henkelman, J. Phys.: Condens. Matter **21**, 084204 (2009).

[8] G. Kresse and J. Furthmüller, Phys. Rev. B **54**, 11169 (1996).

[9] J. P. Perdew, K. Burke, and Y. Wang, Phys. Rev. B **54**, 16533 (1996).

[10] P. E. Blöchl, Phys. Rev. B **50**, 17953 (1994).

[11] H. J. Monkhorst and J. D. Pack, Phys. Rev. B **13**, 5188 (1972).

[12] F. Birch, Phys. Rev. **71**, 809 (1947).

[13] J.F. Nye, Physical Properties of Crystals, Their Representation by Tensors and Matrices, Oxford Press, Chap. VIII, 1957.

[14] W. Voigt, *Lehrburch der Kristallphysik* (Teubner, Leipzig, 1928).

[15] A. Reuss and Z. Angew, Math. Mech. **9**, 49 (1929).

[16] R. Hill, Phys. Phys. Soc. London **65**, 349 (1952).

[17] J. Hanies, J. M. Leger, and G. Bocquillon, Annu. Rev. Mater. Res. **31**, 1 (2001).

[18] J. P. Watt and L. Peselnick, J. Appl. Phys. **51**, 1525 (1980).

[19] C. Keller, *Thorium* (Springer, 1978).

[20] W. H. Zachariasen, Acta Cryst. **6**, 395 (1953).

[21] J. H. Weaver, J. A. Knapp, D. E. Eastman, D. T. Peterson, and C. B. Satterthwaite, Phys. Rev. Lett. **39**, 639 (1977).

[22] B. Wang, H, Shi, W. Li, and P. Zhang, aiXiv:0908.3558v1 [cond-mat.mtrl-sci] (2009).

[23] J. F. Nye, *Physical Properties of Crystals* (Oxford University Press, Oxford, 1985).